Received: 23 December 2018 | Accepted: 4 June 2019

DOI: 10.1002/rnc.4659

RESEARCH ARTICLE

WILEY

Robust adaptive trajectory tracking control of underactuated autonomous underwater vehicles with prescribed performance

Jian Li[1] | **Jialu Du**[1] | **Yuqing Sun**[2] | **Frank L. Lewis**[3]

[1]National Center for International Research of Subsea Engineering Technology and Equipment, School of Marine Electrical Engineering, Dalian Maritime University, Dalian, China

[2]National Center for International Research of Subsea Engineering Technology and Equipment, School of Marine Engineering, Dalian Maritime University, Dalian, China

[3]Automation and Robotics Research Institute, University of Texas at Arlington, Arlington, Texas

Correspondence
Jialu Du, National Center for International Research of Subsea Engineering Technology and Equipment, School of Marine Engineering, Dalian Maritime University, Dalian, Liaoning 116026, China.
Email: dujl66@163.com

Funding information
National Natural Science Foundation of China, Grant/Award Number: 51079013

Summary

In this paper, a novel robust adaptive trajectory tracking control scheme with prescribed performance is developed for underactuated autonomous underwater vehicles (AUVs) subject to unknown dynamic parameters and disturbances. A simple error mapping function is proposed in order to guarantee that the trajectory tracking error satisfies the prescribed performance. A novel additional control based on Nussbaum function is proposed to handle the underactuation of AUVs. The compounded uncertain item caused by the unknown dynamic parameters and disturbances is transformed into a linear parametric form with only single unknown parameter called virtual parameter. On the basis of the above, a novel robust adaptive trajectory tracking control law is developed using dynamic surface control technique, where the adaptive law online provides the estimation of the virtual parameter. Strict stability analysis indicates that the designed control law ensures uniform ultimate boundedness of the AUV trajectory tracking closed-loop control system with prescribed tracking performance. Simulation results on an AUV in two different disturbance cases with dynamic parameter perturbation verify the effectiveness of our adaptive trajectory tracking control scheme.

KEYWORDS

additional control, autonomous underwater vehicle, prescribed performance, robust adaptive control, virtual parameter

1 | INTRODUCTION

The last decades have witnessed tremendous progress in the development of marine technologies that are steadily affording scientists advanced equipment and methods for ocean exploration and exploitation. Recent advances in marine robotics, sensors, computers, communications, and information systems are being applied to the development of sophisticated technologies that will lead to safer, faster, and far more efficient ways of exploring the ocean frontier, especially in hazardous environment. In recent years, there has been a surge of worldwide interest in the development of autonomous marine robots with the capability of roaming the oceans freely and collecting data underwater on an unprecedented scale.[1-4] Representative examples are autonomous underwater vehicles (AUVs). The trajectory tracking problem of the AUVs has received considerable attentions.[5-8]

The AUVs have the characteristics of highly nonlinearity, parameter uncertainty, and others in dynamics and are exposed to unpredictable underwater environment, which puts considerable challenges in the trajectory tracking control

design. Various control techniques have been used to solve the trajectory tracking control problem of AUVs with unknown dynamic parameters and disturbances, such as adaptive control,[9] sliding mode control,[10,11] neural network (NN),[12,13] robust integral of the sign of the error technique,[14] disturbance observer-based control,[15] and adding a power integrator-based method.[16] All the AUVs considered in the literature[9-16] are fully actuated.

However, the number of actuators of AUVs is mostly fewer than the number of freedom degrees of their movement in practice, which means that AUVs are mostly underactuated. So far, the tracking control of underactuated AUVs has received a considerable amount of attentions. For the trajectory tracking of underactuated AUVs with unknown hydrodynamic damping terms and bounded disturbances, Park[17] proposed an additional control method together with an approach angle to deal with the underactuation of the AUVs and designed an adaptive NN tracking control law. In the presence of unmodeled dynamics and environmental disturbances, Elmokadem et al[18] used the second derivative of the sway velocity to overcome the underactuation of the AUVs and designed a terminal sliding mode trajectory tracking control law. For the underactuated AUV subject to actuator saturation and external disturbances, an adaptive fuzzy trajectory tracking control scheme was proposed in the work of Yu et al.[19] For the underactuated AUVs subject to model uncertainties and environmental disturbances, the robust trajectory tracking control schemes are presented, incorporating the NN into feedback linearization technique[20] and the dynamic surface control (DSC) technique,[21] respectively. For path tracking of underactuated AUVs with unknown parameters and environmental disturbances, Do et al[22] proposed a robust adaptive control strategy based on backstepping method and parameter projection technique[23] and designed a robust control scheme combining the fuzzy algorithm with feedback linearization technique. In the works,[19-23] the light-of-sight (LOS) guidance method was employed to deal with the underactuation of the AUVs. Moreover, Caharija et al[24] proposed an integral LOS guidance method and designed a nonlinear control law for path following of underactuated AUVs in the presence of ocean current disturbances.

On the other hand, from a practical point of view, it is important to take the prescribed transient and steady-state control performance account into the control design. Bechlioulis and Rovithakis[25] proposed the prescribed performance control method, where the logarithmic error mapping function was constructed so as to achieve the prescribed performance control. This method has been employed to the prescribed performance tracking control for several classes of nonlinear systems[26-28] and for underactuated AUVs[29-31] or surface vessels,[32,33] receptively. However, the logarithmic error mapping functions used in related works[25-33] lead to the potential singularity problem of the designed control laws.[34] In order to avoid this problem, Han and Lee[34] and Wang and Yang[35] constructed the nonlogarithmic piecewise error mapping functions to achieve the prescribed performance control for a class of strict-feedback nonlinear systems and a class of MIMO nonlinear systems, respectively.

Motivated by the aforementioned discussion, we propose a novel robust adaptive prescribed performance trajectory tracking control scheme for underactuated AUVs subject to unknown dynamic parameters and disturbances. The main contributions in this paper lie in as follows.

i. A novel additional control based on Nussbaum function is proposed to handle the underactuation of the AUV, which discards the assumption on the passive-boundedness of sway velocity in other works.[20,21,32] Furthermore, the introduction of the additional control results in that the tracking control law for the underactuated AUV in this paper can be designed in a vector setting such that the design process is simplified and well suited for computer implementation.
ii. The compounded uncertain item caused by the unknown dynamic parameters and disturbances is transformed into a linear parametric form with only single unknown parameter such that the computational burden of the designed resulting control scheme is largely reduced in contrast to related works.[9,12,13,19]
iii. A simple nonlogarithmic error mapping function is proposed to guarantee that the trajectory tracking error satisfies the prescribed performance such that a potential singularity problem of the developed control scheme is avoided.

The remaining parts of this paper are organized as follows. Section 2 introduces the problem formulation and preliminaries. Section 3 proposes the control design procedures. Section 4 contains the simulations to show the effectiveness of the proposed control scheme. Section 5 concludes the paper.

Notation. Throughout this paper, $\|\cdot\|$ denotes the 2-norm of a vector or a matrix, $\lambda_{\min}(\cdot)$ denotes the minimum eigenvalue of a matrix, and diag$(\cdot)$ denotes a dialog matrix. For any vector $\boldsymbol{a} \in \boldsymbol{R}^n$, a_j denotes the jth element of the vector. For a diagonal matrix $\boldsymbol{b} \in \boldsymbol{R}^{n\times n}$, b_j denotes the jth element on the main diagonal of the diagonal matrix.

2 | PROBLEM FORMULATION AND PRELIMINARIES

2.1 | AUV's mathematical model

We consider the trajectory tracking of AUVs in the horizontal plane for constant depth applications, such as seabed surveys. It is assumed that the shape of AUVs is symmetrical with respect to both xz-plane and yz-plane in the body-fixed frame. Neglecting the motions in heave, roll, and pitch, the mathematical model of AUVs can be described as[4]

$$\dot{\boldsymbol{\eta}} = \boldsymbol{J}(\psi)\boldsymbol{\upsilon} \tag{1}$$

$$\boldsymbol{M}\dot{\boldsymbol{\upsilon}} + \boldsymbol{C}(\boldsymbol{\upsilon})\boldsymbol{\upsilon} + \boldsymbol{D}(\boldsymbol{\upsilon})\boldsymbol{\upsilon} = \boldsymbol{\tau} + \boldsymbol{d}(t), \tag{2}$$

where $\boldsymbol{\eta} = [x, y, \psi]^{\mathrm{T}}$ is the position vector of the AUV in the earth-fixed frame, consisting of the position (x, y) and yaw angle $\psi \in [0, 2\pi)$. $\boldsymbol{\upsilon} = [u, v, r]^{\mathrm{T}}$ is the velocity vector of the AUV in the body-fixed frame, consisting of the surge velocity u, the sway velocity v, and the yaw rate r of the AUV. $\boldsymbol{J}(\psi)$ is the rotation matrix, $\boldsymbol{M}$ is the positive definite inertia matrix, $\boldsymbol{C}(\boldsymbol{\upsilon})$ is the matrix of Coriolis and centripetal terms, and $\boldsymbol{D}(\boldsymbol{\upsilon})$ is the damping matrix. They are, respectively, $\boldsymbol{J}(\psi) = \begin{bmatrix} \cos(\psi) & -\sin(\psi) & 0 \\ \sin(\psi) & \cos(\psi) & 0 \\ 0 & 0 & 1 \end{bmatrix}$, $\boldsymbol{M} = \begin{bmatrix} m_{1,1} & 0 & 0 \\ 0 & m_{2,2} & 0 \\ 0 & 0 & m_{3,3} \end{bmatrix}$, $\boldsymbol{C}(\boldsymbol{\upsilon}) = \begin{bmatrix} 0 & 0 & -m_{2,2}v \\ 0 & 0 & m_{1,1}u \\ m_{2,2}v & -m_{1,1}u & 0 \end{bmatrix}$, $\boldsymbol{D}(\boldsymbol{\upsilon}) = \begin{bmatrix} d_{1,1}(u) & 0 & 0 \\ 0 & d_{2,2}(v) & 0 \\ 0 & 0 & d_{3,3}(r) \end{bmatrix}$, where $m_{1,1} = m - X_{\dot{u}}, m_{2,2} = m - Y_{\dot{v}}, m_{3,3} = I_z - N_{\dot{r}}, d_{1,1}(u) = -X_u - X_{u|u|}|u|, d_{2,2}(v) = -Y_v - Y_{v|v|}|v|$, and $d_{3,3}(r) = -N_r - N_{r|r|}|r|$. m is the mass of the AUV; $X_{\dot{u}}$, $Y_{\dot{v}}$, and $N_{\dot{r}}$ are the added masses; I_z is the moment of inertia in yaw; and X_u, $X_{u|u|}$, Y_v, $Y_{v|v|}$, N_r, and $N_{r|r|}$ are referred to as hydrodynamic derivatives. $\boldsymbol{\tau} = [\tau_u, 0, \tau_r]^{\mathrm{T}}$ is the control input vector consisting of the surge force, the sway force (which is zero due to the underactuation of the AUV), and the yaw moment. $\boldsymbol{d}(t) = [d_1(t), d_2(t), d_3(t)]^{\mathrm{T}}$ is the disturbance vector.

Assumption 1.

1. The AUV's dynamic parameters $m_{j,j}$ and $d_{j,j}$ $(j = 1, 2, 3)$ are unknown.
2. The environmental disturbance vector $\boldsymbol{d}(t) = [d_1(t), d_2(t), d_3(t)]^{\mathrm{T}}$ is bounded yet unknown time-varying and there exists positive constant $\bar{d}_j$ such that
$$|d_j| \leq \bar{d}_j. \tag{3}$$

Remark 1. The dynamic model parameters of the AUV are related with the AUV's mass, the hydrodynamic derivatives, the moment of inertia about the rotation, and the operating conditions, and are difficult to be determined in practice. On the other hand, the environmental disturbances are always changing, unpredictable, and limited in energy. Therefore, Assumption 1 is reasonable.

Assumption 2. The desired trajectory $\boldsymbol{\eta}_d = [x_d, y_d, \psi_d]^{\mathrm{T}}$ of the AUV and its first two time derivatives are bounded.

2.2 | Control objective

The underactuated AUV (1)-(2) is required to track the desired trajectory with prescribed performance of the tracking error. Define the tracking error $\boldsymbol{e} = [e_x, e_y, e_\psi]^{\mathrm{T}}$ as

$$\boldsymbol{e} = \boldsymbol{\eta} - \boldsymbol{\eta}_\alpha, \tag{4}$$

where $\boldsymbol{\eta}_\alpha = [x_d, y_d, \psi_\alpha]^{\mathrm{T}}$, ψ_α is the $\eta_\alpha = [x_d, y_d, \psi_\alpha]^{\mathrm{T}}$ approach angle given by[17,32]

$$\psi_\alpha = \operatorname{atan2}(e_y, e_x) \tanh\left(\left(e_x^2 + e_y^2\right)/\delta\right) + \psi_d\left(1 - \tanh\left(\left(e_x^2 + e_y^2\right)/\delta\right)\right). \tag{5}$$

The approach angle is employed to help handle the underactuation of the AUV. It can be known from (5) that $\psi_\alpha = \psi_d$ when $e_x = e_y = 0$, which means that the AUV will track the desired trajectory when the tracking error e converge to zero or near to zero.

To achieve the prescribed trajectory tracking control performance of the AUV, the tracking error should satisfy the following inequality:

$$-\underline{e}_j(t) < e_j(t) < \bar{e}_j(t), \forall t \geq 0, j = x, y, \psi, \tag{6}$$

with

$$\bar{e}_j(t) = \left(\bar{e}_{j,0} - \bar{e}_{j,\infty}\right)\exp\left(-\mu_j t\right) + \bar{e}_{j,\infty} \tag{7}$$

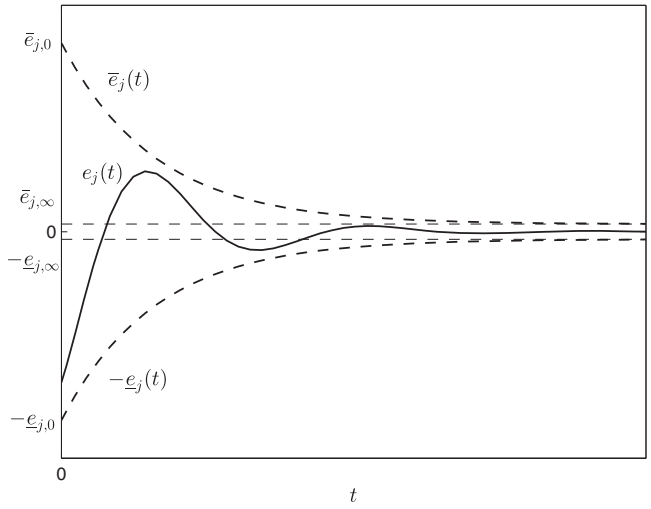

FIGURE 1 Graphical illustration of prescribed performance

$$\underline{e}_j(t) = \left(\underline{e}_{j,0} - \underline{e}_{j,\infty}\right) \exp\left(-\mu_j t\right) + \underline{e}_{j,\infty}, \tag{8}$$

where $\bar{e}_{j,0}$, $\bar{e}_{j,\infty}$, μ_j, $\underline{e}_{j,0}$, and $\underline{e}_{j,\infty}$ are positive constants. $\bar{e}_{j,\infty}$ and $\underline{e}_{j,\infty}$ are the maximum allowable steady-state tracking error with $\bar{e}_{j,\infty} \leq \bar{e}_{j,0}$ and $e_{j,\infty} \leq \underline{e}_{j,0}$, and μ_j represents the convergence speed of $e_j(t)$, as illustrated in Figure 1. Note that $\bar{e}_j(t)$ and $\underline{e}_j(t)$ are exponentially decaying functions. Inequality (6) represents the prescribed performance of the AUV tracking errors.

The control objective in this paper is to develop a robust adaptive tracking control law for the underactuated AUV (1)-(2) under Assumptions 1 and 2, such that the AUV tracks the desired trajectory $\boldsymbol{\eta}_d = [x_d, y_d, \psi_d]^{\mathrm{T}}$ with the tracking error e_j settling within the prescribed boundaries $\underline{e}_j(t)$ and $\bar{e}_j(t)$, whereas all signals in the closed-loop tracking control system are guaranteed uniformly ultimately bounded.

2.3 | Preliminaries

Definition 1 (See the work of Nussbaum[36]). A differentiable function $N(\kappa)$ is called a Nussbaum-type function if it has the following properties:

$$\limsup_{s\to\infty} \frac{1}{s} \int_0^s N(\kappa) d\kappa = +\infty \tag{9}$$

$$\liminf_{s\to\infty} \frac{1}{s} \int_0^s N(\kappa) d\kappa = -\infty. \tag{10}$$

The lemma regarding the property of Nussbaum function is given as follows.

Lemma 1. (See the work of Wen et al[37]). *Let $N(\kappa)$ be an even Nussbaum function, $V(\cdot)$ and $\kappa(\cdot)$ be smooth functions defined on $[0, t_f)$, with $V(t) \geq 0$, $\forall t \in [0, t_f)$. If the following inequality holds:*

$$V \leq \frac{C}{2\mu} + \left[V(0) - \frac{C}{2\mu}\right] e^{-2\mu t} + \frac{\exp^{-2\mu t}}{\gamma_\chi} \int_0^t \sum_{i=1}^{n} \left(\theta_i N(\kappa_i) - 1\right) \dot{\kappa}_i \exp^{2\mu s} ds, \tag{11}$$

where $\mu > 0$, $\gamma_\chi > 0$, $\theta > 0$, C is a positive constant, then $V(\cdot)$, $\kappa(\cdot)$, and $\int_0^t \sum_{i=1}^{n} (\theta_i N(\kappa_i) - 1)\dot{\kappa}_i \exp^{2\mu s} ds$ are bounded on $[0, t_f)$.

Commonly used Nussbaum functions include $\kappa^2 \cos(\kappa)$, $\kappa^2 \sin(\kappa)$, and $\exp(\kappa^2)\cos((\pi/2)\kappa)$.

Proposition 1. (See the work of Ryan[38]). *For the general initial-value problem*

$$\dot{h}(t) \in F\left(h(t)\right), h(t) \in R^n \tag{12}$$

$$h(0) = h^0, \tag{13}$$

where $F(h) : R^n \to R^n$ is continuous. Suppose $0 < \omega \leq \infty$ and that $h : [0, \omega) \to R^n$ is a bounded solution of (12), then $\omega = \infty$.

Remark 2. From Proposition 1, if the solution of a closed-loop system is bounded, then, for each $h^0 \in R^n$, no finite-time escape phenomenon may happen and the result of the boundedness on $[0, t_f)$ in Lemma 1 is able to be extended to $t_f = \infty$.

3 | ROBUST ADAPTIVE TRAJECTORY TRACKING CONTROL DESIGN

In this section, we design a robust adaptive trajectory tracking control law for the underactuated AUV (1)-(2) to achieve the control objective in Section 2.2. To ensure the tracking error satisfying the requirements of the prescribed performance (6), we construct a simple error mapping function. Novel additional control is proposed to handle the underactuation problem of AUVs. Then, we design a robust adaptive trajectory tracking control law using a linear parametric transformation and the DSC technique.[39]

First, we construct the error mapping function as follows:

$$z_{1,j} = f\left(e_j, \bar{e}_j, \underline{e}_j\right) = \frac{e_j}{\left(\bar{e}_j - e_j\right)\left(e_j + \underline{e}_j\right)}, \tag{14}$$

where the transform variable $z_{1,j}$ is equivalent to the tracking error e_j.

Remark 3. It is seen from (14) that the transform variable $z_{1,j}$ will approach infinity when the tracking error e_j approaches its prescribed boundaries $\bar{e}_j$ or $\underline{e}_j$. Thus, the error mapping function transforms the tracking error constraint problem of AUV trajectory tracking into the problem of the boundedness of transform variable. Since $f(\cdot)$ in (14) is strictly increasing, it follows that, if $z_{1,j}$ is guaranteed to be bounded under the initial condition $-\underline{e}_j(0) < e_j(0) < \bar{e}_j(0)$, the prescribed performance (6) of the tracking error is guaranteed. Besides, in some literature, the error transformation function $f(\cdot)$ was chosen as a logarithmic function, which would cause the potential singularity problem of the control law. In this paper, our proposed error mapping function (14) can avoid this problem.

Then, we design the robust adaptive trajectory tracking control law of the underactuated AUV.

Step 1: Taking the derivative of $z_{1,j}$ on both sides of (14), we have

$$\begin{aligned}\dot{z}_{1,j} &= \frac{\dot{e}_j\left(\bar{e}_j - e_j\right)\left(e_j + \underline{e}_j\right) - e_j\left[\left(\dot{\bar{e}}_j - \dot{e}_j\right)\left(e_j + \underline{e}_j\right) + \left(\bar{e}_j - e_j\right)\left(\dot{e}_j + \dot{\underline{e}}_j\right)\right]}{\left(\bar{e}_j - e_j\right)^2\left(e_j + \underline{e}_j\right)^2} \\ &= P_j\dot{e}_j + Q_j.\end{aligned} \tag{15}$$

where $P_j = \left[\frac{e_j^2 + \bar{e}_j\underline{e}_j}{(\bar{e}_j - e_j)^2(e_j + \underline{e}_j)^2}\right] > 0$ and $Q_j = \left[\frac{-e_j^2(\dot{\bar{e}}_j - \dot{e}_j) - e_j(\dot{\bar{e}}_j\underline{e}_j + \bar{e}_j\dot{\underline{e}}_j)}{(\bar{e}_j - e_j)^2(e_j + \underline{e}_j)^2}\right]$.

According to (1), (2), (4), and (15), we have

$$\dot{\boldsymbol{z}}_1 = \boldsymbol{P}\left[\boldsymbol{J}(\psi)\boldsymbol{\upsilon} - \dot{\boldsymbol{\eta}}_\alpha\right] + \boldsymbol{Q}, \tag{16}$$

where $\boldsymbol{P} = \mathrm{diag}(P_1, P_2, P_3) \in \boldsymbol{R}^{3\times3}$, $\boldsymbol{Q} = [Q_1, Q_2, Q_3]^{\mathrm{T}} \in \boldsymbol{R}^3$, and $\boldsymbol{\upsilon}$ is viewed as the virtual control input.

Design the intermediate control $\boldsymbol{\alpha} \in \boldsymbol{R}^3$ for $\boldsymbol{\upsilon}$ as follows:

$$\boldsymbol{\alpha} = \boldsymbol{J}^{\mathrm{T}}(\psi)\left[\boldsymbol{P}^{-1}\left(-\boldsymbol{K}_1\boldsymbol{z}_1 - \boldsymbol{Q}\right) + \dot{\boldsymbol{\eta}}_\alpha - \boldsymbol{P}\boldsymbol{z}_1\right], \tag{17}$$

where $\boldsymbol{K}_1 \in \boldsymbol{R}^{3\times3}$ is a positive-definite design matrix.

Let $\boldsymbol{\alpha}$ pass through the following first-order filter

$$T_d\dot{\boldsymbol{X}}_d + \boldsymbol{X}_d = \boldsymbol{\alpha}; \boldsymbol{X}_d(0) = \boldsymbol{\alpha}(0), \tag{18}$$

where $\boldsymbol{X}_d \in \boldsymbol{R}^3$ is the state vector of the first-order filter and T_d is a positive design constant.

Step 2: Define the new error vector

$$\boldsymbol{z}_2 = \boldsymbol{\upsilon} - \boldsymbol{X}_d. \tag{19}$$

The time derivative of (19) along (2) is

$$\dot{\boldsymbol{z}}_2 = \boldsymbol{M}^{-1}\left[-\boldsymbol{C}(\boldsymbol{\upsilon})\boldsymbol{\upsilon} - \boldsymbol{D}(\boldsymbol{\upsilon})\boldsymbol{\upsilon} + \boldsymbol{\tau} + \boldsymbol{d}(t) - \boldsymbol{M}\dot{\boldsymbol{X}}_d\right]. \tag{20}$$

Let

$$\boldsymbol{L}(\boldsymbol{\rho}) = \boldsymbol{M}^{-1}\left[-\boldsymbol{C}(\boldsymbol{\upsilon})\boldsymbol{\upsilon} - \boldsymbol{D}(\boldsymbol{\upsilon})\boldsymbol{\upsilon} + \boldsymbol{d}(t) - \boldsymbol{M}\dot{\boldsymbol{X}}_d\right], \tag{21}$$

with $\boldsymbol{\rho} = [\boldsymbol{\upsilon}^{\mathrm{T}}, \dot{\boldsymbol{X}}_d^{\mathrm{T}}]^{\mathrm{T}}$. $\boldsymbol{L}(\boldsymbol{\rho})$ is equivalently the compounded uncertain item caused by the unknown dynamic parameters and disturbances. For the convenience of later control design, we take the following transformation:

$$\boldsymbol{C}(\boldsymbol{\upsilon})\boldsymbol{\upsilon} + \boldsymbol{M}\dot{\boldsymbol{X}}_d = \boldsymbol{\phi}_1\left(\boldsymbol{\upsilon}, \dot{\boldsymbol{X}}_d\right)\boldsymbol{C}_m \tag{22}$$

$$\boldsymbol{D}(\boldsymbol{\upsilon})\boldsymbol{\upsilon} = \boldsymbol{\phi}_2(\boldsymbol{\upsilon})\boldsymbol{D}_{m1} + \boldsymbol{\phi}_3(\boldsymbol{\upsilon})\boldsymbol{D}_{m2}, \tag{23}$$

where $\boldsymbol{\phi}_1(\boldsymbol{\upsilon}, \dot{\boldsymbol{X}}_d) = \begin{bmatrix} \dot{X}_{d,1} & -vr & 0 \\ ur & \dot{X}_{d,2} & 0 \\ -uv & uv & \dot{X}_{d,3} \end{bmatrix}$, $\boldsymbol{C}_m = [m_{1,1}, m_{2,2}, m_{3,3}]^{\mathrm{T}}$, $\boldsymbol{\phi}_2(\boldsymbol{\upsilon}) = \mathrm{diag}(u, v, r)$, $\boldsymbol{D}_{m1} = [-X_u, -Y_v, -N_r]^{\mathrm{T}}$, $\boldsymbol{\phi}_3(\boldsymbol{\upsilon}) = \mathrm{diag}(u|u|, v|v|, r|r|)$, and $\boldsymbol{D}_{m2} = [-X_{|u|u}, -Y_{|v|v}, -N_{|r|r}]^{\mathrm{T}}$.

According to (21)-(23), we further make the following linear parametric transformation:

$$\begin{aligned} \|\boldsymbol{L}(\boldsymbol{\rho})\| &\le \left\|\boldsymbol{M}^{-1}\right\|\left(\left\|\boldsymbol{C}(\boldsymbol{\upsilon})\boldsymbol{\upsilon} + \boldsymbol{M}\dot{\boldsymbol{X}}_d\right\| + \|\boldsymbol{D}(\boldsymbol{\upsilon})\boldsymbol{\upsilon}\| + \left\|\overline{\boldsymbol{d}}\right\|\right) \\ &\le \left\|\boldsymbol{M}^{-1}\right\|\left(\left\|\boldsymbol{\phi}_1\left(\boldsymbol{\upsilon}, \dot{\boldsymbol{X}}_d\right)\boldsymbol{C}_m\right\| + \left\|\boldsymbol{\phi}_2(\boldsymbol{\upsilon})\boldsymbol{D}_{m1} + \boldsymbol{\phi}_3(\boldsymbol{\upsilon})\boldsymbol{D}_{m2}\right\| + \left\|\overline{\boldsymbol{d}}\right\|\right) \\ &\le \left\|\boldsymbol{M}^{-1}\right\|\left\|\boldsymbol{\phi}_1\left(\boldsymbol{\upsilon}, \dot{\boldsymbol{X}}_d\right)\right\|\|\boldsymbol{C}_m\| + \left\|\boldsymbol{M}^{-1}\right\|\|\boldsymbol{\phi}_2(\boldsymbol{\upsilon})\|\,\boldsymbol{D}_{m1}\| + \|\boldsymbol{M}^{-1}\|\left\|\boldsymbol{\phi}_3(\boldsymbol{\upsilon})\right\|\|\boldsymbol{D}_{m2}\| + \left\|\boldsymbol{M}^{-1}\right\|\left\|\overline{\boldsymbol{d}}\right\| \\ &\le \Theta^*\phi\left(\|\boldsymbol{\rho}\|\right), \end{aligned} \tag{24}$$

where $\Theta^* = \max\left\{\|\boldsymbol{M}^{-1}\|\|\boldsymbol{C}_m\|, \|\boldsymbol{M}^{-1}\|\|\boldsymbol{D}_{m1}\|, \|\boldsymbol{M}^{-1}\|\|\boldsymbol{D}_{m2}\|, \|\boldsymbol{M}^{-1}\|\|\overline{\boldsymbol{d}}\|\right\}$ and $\phi(\|\boldsymbol{\rho}\|) = \|\boldsymbol{\phi}_1(\boldsymbol{\upsilon}, \dot{\boldsymbol{X}}_d)\| + \|\boldsymbol{\phi}_2(\boldsymbol{\upsilon})\| + \|\boldsymbol{\phi}_3(\boldsymbol{\upsilon})\| + 1$. Since Θ^* has not a clear physical significance, herein it is called the virtual parameter.[40]

Remark 4. There are actually nine unknown parameters in $\boldsymbol{L}(\boldsymbol{\rho})$. Definitely, estimating all these parameters will bring the great computational burden and tuning the design gain of estimators is also difficult. By means of the linear parametric transformation (24), only single unknown parameter needs to be online updated, instead of actual nine unknown parameters, such that the computational burden of the designed resulting control scheme is largely reduced.

Furthermore, we proposed a novel additional control to handle the underactuation of the AUV. The error vector (19) is firstly changed into a new one with the additional control vector $\boldsymbol{T}(\lambda) = [0, \tanh(\lambda_2), 0]^{\mathrm{T}}$

$$\overline{\boldsymbol{z}}_2 = \boldsymbol{\upsilon} - \boldsymbol{X}_d + K_2\boldsymbol{T}(\lambda), \tag{25}$$

where K_2 is a positive design constant, and $\lambda = [0, \lambda_2, 0]^{\mathrm{T}}$ is the state vector of the following auxiliary dynamic system:

$$\dot{\lambda} = K_2^{-1}(-\gamma\lambda + \xi) \tag{26}$$

$$\xi = \boldsymbol{N}\overline{\xi} \tag{27}$$

$$\overline{\xi} = -\boldsymbol{L}_1\boldsymbol{K}_3\overline{\boldsymbol{z}}_2 + \boldsymbol{L}_1\left[-\boldsymbol{J}^{\mathrm{T}}(\psi)\boldsymbol{P}\boldsymbol{z}_1 - \hat{\Theta}\phi^2\left(\|\boldsymbol{\rho}\|\right)\overline{\boldsymbol{z}}_2\right] + \gamma\boldsymbol{\Lambda}\lambda. \tag{28}$$

Here, γ is a positive design constant, $\xi \in \boldsymbol{R}^3$ is the intermediate vector, $\boldsymbol{L}_1 = \begin{bmatrix} 0 & 0 & 0 \\ 0 & 1 & 0 \\ 0 & 0 & 0 \end{bmatrix}$ is a coefficient matrix, $\boldsymbol{K}_3 = \begin{bmatrix} K_{3,11} & K_{3,12} & 0 \\ -K_{3,12} & K_{3,22} & -K_{3,23} \\ 0 & K_{3,23} & K_{3,33} \end{bmatrix}$ is a design matrix with $K_{3,ij} > 0$, $\hat{\Theta}$ is the estimate of Θ^*, and $\boldsymbol{\Lambda} = \mathrm{diag}(0, \Lambda_2, 0)$ with $\Lambda_2 = \frac{d[\tanh(\lambda_2)]}{d(\lambda_2)}$. $\boldsymbol{N} = \mathrm{diag}(0, N_2(\chi_2), 0)$, where $N_2(\chi_2)$ is the Nussbaum function given by

$$N_2(\chi_2) = \chi_2^2\cos(\chi_2) \tag{29}$$

with

$$\dot{\chi}_2 = \gamma_\chi \bar{z}_{2,2} \bar{\xi}_2, \tag{30}$$

where γ_χ is a positive design constant.

According to (2), (21), (26)-(28), taking the time derivative of $\bar{\boldsymbol{z}}_2$ yields

$$\begin{aligned} \dot{\bar{\boldsymbol{z}}}_2 &= \dot{\boldsymbol{\upsilon}} - \dot{\boldsymbol{X}}_d + K_2 \boldsymbol{\Lambda} \dot{\boldsymbol{\lambda}} \\ &= \boldsymbol{M}^{-1} \boldsymbol{\tau} + \boldsymbol{L}(\boldsymbol{\rho}) - \gamma \boldsymbol{\Lambda} \boldsymbol{\lambda} + \boldsymbol{\Lambda} \boldsymbol{\xi} \\ &= \boldsymbol{M}^{-1} \boldsymbol{\tau} + \boldsymbol{L}(\boldsymbol{\rho}) + \boldsymbol{L}_1 \boldsymbol{K}_3 \bar{\boldsymbol{z}}_2 + \boldsymbol{L}_1 \left[-\boldsymbol{J}^{\mathrm{T}}(\psi) \boldsymbol{P} \boldsymbol{z}_1 - \hat{\Theta} \phi^2 (\|\boldsymbol{\rho}\|) \bar{\boldsymbol{z}}_2 \right] - \bar{\boldsymbol{\xi}} + \boldsymbol{\Lambda} \boldsymbol{\xi}. \end{aligned} \tag{31}$$

Remark 5. The proposed additional control vector $\boldsymbol{T}(\boldsymbol{\lambda})$ in (25) is used to handle the underactuation of the AUV, which not only discards the assumption that the sway velocity is passive-bounded but also designs the trajectory tracking control law for underactuated AUVs in a vector setting instead of in a component form. From a computational point of view, the vectorial control law is beneficial thanks to the compact notation.

Remark 6. A similar study using the additional control can be found in the work of Park and Yoo.[32] However, in the aforementioned work,[32] the term $\cosh^2(\mu_i)$ appears in the auxiliary dynamic systems, which brings the challenge to the boundedness analysis of μ_i and may cause μ_i to rapidly reach infinite due to the big changing rate of $\cosh^2(\mu_i)$. In this paper, we introduce the Nussbaum function to the additional control $\boldsymbol{T}(\boldsymbol{\lambda})$ by means of the auxiliary dynamic system (26), as a result, the challenge of the boundedness analysis of λ_2 is easily solved and the potential infinite problem of λ_2 is avoided. In addition, some other functions similar to Nussbaum functions can be used to design the auxiliary dynamic system, such as nonlinear proportion integration (PI) functions proposed in the works of Wang et al.[41,42]

Design the robust adaptive trajectory tracking control law

$$\begin{aligned} \tau &= \hat{\boldsymbol{M}} \left\{ -\boldsymbol{L}_2 \boldsymbol{K}_3 \bar{\boldsymbol{z}}_2 + \boldsymbol{L}_2 \left[-\boldsymbol{J}^{\mathrm{T}}(\psi) \boldsymbol{P} \boldsymbol{z}_1 - \hat{\Theta} \phi^2 (\|\boldsymbol{\rho}\|) \bar{\boldsymbol{z}}_2 \right] \right\} \\ &= \hat{\boldsymbol{M}} \bar{\boldsymbol{\tau}} \end{aligned} \tag{32}$$

with adaptive laws

$$\dot{\hat{m}}_{j,j} = -H_j \left(\bar{\tau}_j \bar{z}_{2,j} + \Omega_j \hat{m}_{j,j} \right), j = 1, 2, 3 \tag{33}$$

$$\dot{\hat{\Theta}} = \Gamma \left[\phi^2 (\|\boldsymbol{\rho}\|) \left\| \bar{\boldsymbol{z}}_2 \right\|^2 - \sigma \hat{\Theta} \right], \tag{34}$$

where $\hat{\boldsymbol{M}} = \mathrm{diag}(\hat{m}_{1,1}, \hat{m}_{2,2}, \hat{m}_{3,3})$ is the estimation of $\boldsymbol{M}$, $\bar{\boldsymbol{\tau}} = [\bar{\tau}_1, \bar{\tau}_2, \bar{\tau}_3]^{\mathrm{T}} = -\boldsymbol{L}_2 \boldsymbol{K}_3 \bar{\boldsymbol{z}}_2 + \boldsymbol{L}_2 [-\boldsymbol{J}^{\mathrm{T}}(\psi) \boldsymbol{P} \boldsymbol{z}_1 - \hat{\Theta} \phi^2 (\|\boldsymbol{\rho}\|) \bar{\boldsymbol{z}}_2]$, $\boldsymbol{L}_2 = \begin{bmatrix} 1 & 0 & 0 \\ 0 & 0 & 0 \\ 0 & 0 & 1 \end{bmatrix}$ is a design matrix, and H_j, Ω_j, Γ, and σ are the positive design constants.

Select the following Lyapunov function candidate for the whole system consisting of (1), (2), (17), (18), (26)-(28), (32)-(34) as

$$V = \frac{1}{2} \left(\boldsymbol{z}_1^{\mathrm{T}} \boldsymbol{z}_1 + \bar{\boldsymbol{z}}_2^{\mathrm{T}} \bar{\boldsymbol{z}}_2 + \boldsymbol{Y}_2^{\mathrm{T}} \boldsymbol{Y}_2 + \sum_{j=1}^{3} m_{j,j}^{-1} H_j^{-1} \tilde{m}_{j,j}^2 + \Gamma^{-1} \tilde{\Theta}^2 \right), \tag{35}$$

where $\boldsymbol{Y}_2 = \boldsymbol{X}_d - \boldsymbol{\alpha}$ is the filter error vector, $\tilde{m}_{j,j} = \hat{m}_{j,j} - m_{j,j}$ and $\tilde{\Theta} = \hat{\Theta} - \Theta^*$ are the estimate errors.

The time derivative of V is

$$\dot{V} = \boldsymbol{z}_1^{\mathrm{T}} \dot{\boldsymbol{z}}_1 + \bar{\boldsymbol{z}}_2^{\mathrm{T}} \dot{\bar{\boldsymbol{z}}}_2 + \boldsymbol{Y}_2^{\mathrm{T}} \dot{\boldsymbol{Y}}_2 + \sum_{j=1}^{3} m_{j,j}^{-1} H_j^{-1} \tilde{m}_{j,j} \dot{\hat{m}}_{j,j} + \tilde{\Theta} \Gamma^{-1} \dot{\hat{\Theta}}. \tag{36}$$

According to (16), (17), (25), $\boldsymbol{Y}_2 = \boldsymbol{X}_d - \boldsymbol{\alpha}$, Young's inequality, and the property of the hyperbolic tangent function $\tanh(\cdot)$, we have

$$\begin{aligned}
\boldsymbol{z}_1^{\mathrm{T}}\dot{\boldsymbol{z}}_1 &= \boldsymbol{z}_1^{\mathrm{T}}\{\boldsymbol{P}[\boldsymbol{J}(\psi)(\bar{\boldsymbol{z}}_2 + \boldsymbol{Y}_2 + \boldsymbol{\alpha} - K_2\boldsymbol{T}(\lambda)) - \dot{\boldsymbol{\eta}}_\alpha] + \boldsymbol{Q}\} \\
&\le -\boldsymbol{z}_1^{\mathrm{T}}\boldsymbol{K}_1\boldsymbol{z}_1 + \bar{\boldsymbol{z}}_1^{\mathrm{T}}\boldsymbol{P}\boldsymbol{J}(\psi)\bar{\boldsymbol{z}}_2 + \bar{\boldsymbol{z}}_1^{\mathrm{T}}\boldsymbol{P}\boldsymbol{J}(\psi)\boldsymbol{Y}_2 - K_2\boldsymbol{z}_1^{\mathrm{T}}\boldsymbol{P}\boldsymbol{J}(\psi)\boldsymbol{T}(\lambda) - \boldsymbol{z}_1^{\mathrm{T}}\boldsymbol{P}\boldsymbol{P}\boldsymbol{z}_1 \\
&\le -\boldsymbol{z}_1^{\mathrm{T}}\boldsymbol{K}_1\boldsymbol{z}_1 + \bar{\boldsymbol{z}}_1^{\mathrm{T}}\boldsymbol{P}\boldsymbol{J}(\psi)\bar{\boldsymbol{z}}_2 + \frac{1}{2}\|\bar{\boldsymbol{z}}_1\|^2\|\boldsymbol{P}\|^2 + \frac{1}{2}\|\boldsymbol{Y}_2\|^2 + \frac{1}{2}\|\bar{\boldsymbol{z}}_1\|^2\|\boldsymbol{P}\|^2 + \frac{1}{2}K_2^2 - \boldsymbol{z}_1^{\mathrm{T}}\boldsymbol{P}\boldsymbol{P}\boldsymbol{z}_1 \\
&\le -\boldsymbol{z}_1^{\mathrm{T}}\boldsymbol{K}_1\boldsymbol{z}_1 + \bar{\boldsymbol{z}}_2^{\mathrm{T}}\boldsymbol{P}\boldsymbol{J}(\psi)\bar{\boldsymbol{z}}_2 + \frac{1}{2}\|\boldsymbol{Y}_2\|^2 + \frac{1}{2}K_2^2.
\end{aligned} \tag{37}$$

Note that $\boldsymbol{L}_1 + \boldsymbol{L}_2 = \boldsymbol{I}$ with $\boldsymbol{I}$ being a unit matrix, according to (24), (25), (28)-(30), (32), and Young's inequality, we have

$$\begin{aligned}
\bar{\boldsymbol{z}}_2^{\mathrm{T}}\dot{\bar{\boldsymbol{z}}}_2 &= \bar{\boldsymbol{z}}_2^{\mathrm{T}}\left\{\boldsymbol{M}^{-1}\left(\tilde{\boldsymbol{M}} + \boldsymbol{M}\right)\bar{\boldsymbol{\tau}} + \boldsymbol{L}(\boldsymbol{\rho}) - \boldsymbol{L}_1\boldsymbol{K}_3\bar{\boldsymbol{z}}_2 + \boldsymbol{L}_1\left[-\boldsymbol{J}^{\mathrm{T}}(\psi)\boldsymbol{P}\boldsymbol{z}_1 + \hat{\Theta}\phi^2(\|\boldsymbol{\rho}\|)\bar{\boldsymbol{z}}_2\right] - \bar{\boldsymbol{\xi}} + \boldsymbol{\Lambda}\boldsymbol{\xi}\right\} \\
&\le \|\bar{\boldsymbol{z}}_2\|\|\boldsymbol{L}(\boldsymbol{\rho})\| + \bar{\boldsymbol{z}}_2^{\mathrm{T}}\left\{\boldsymbol{M}^{-1}\left(\tilde{\boldsymbol{M}} + \boldsymbol{M}\right)\bar{\boldsymbol{\tau}} - \boldsymbol{L}_1\boldsymbol{K}_3\bar{\boldsymbol{z}}_2 + \boldsymbol{L}_1\left[-\boldsymbol{J}^{\mathrm{T}}(\psi)\boldsymbol{P}\boldsymbol{z}_1 + \hat{\Theta}\phi^2(\|\boldsymbol{\rho}\|)\bar{\boldsymbol{z}}_2\right]\right\} + \bar{\boldsymbol{z}}_2^{\mathrm{T}}\left(\boldsymbol{\Lambda}\boldsymbol{\xi} - \bar{\boldsymbol{\xi}}\right) \\
&\le \|\bar{\boldsymbol{z}}_2\|\Theta^*\phi(\|\boldsymbol{\rho}\|) + \bar{\boldsymbol{z}}_2^{\mathrm{T}}\left\{\boldsymbol{M}^{-1}\left(\tilde{\boldsymbol{M}} + \boldsymbol{M}\right)\bar{\boldsymbol{\tau}} - \boldsymbol{L}_1\boldsymbol{K}_3\bar{\boldsymbol{z}}_2 + \boldsymbol{L}_1\left[-\boldsymbol{J}^{\mathrm{T}}(\psi)\boldsymbol{P}\boldsymbol{z}_1 + \hat{\Theta}\phi^2(\|\boldsymbol{\rho}\|)\bar{\boldsymbol{z}}_2\right]\right\} + \bar{\boldsymbol{z}}_2^{\mathrm{T}}\left(\boldsymbol{\Lambda}\boldsymbol{\xi} - \bar{\boldsymbol{\xi}}\right) \\
&\le \frac{\Theta^*}{4} + \bar{\boldsymbol{z}}_2^{\mathrm{T}}\left\{-\boldsymbol{I}\boldsymbol{K}_3\bar{\boldsymbol{z}}_2 - \boldsymbol{J}^{\mathrm{T}}(\psi)\boldsymbol{P}\boldsymbol{z}_1 - \tilde{\Theta}\phi^2(\|\boldsymbol{\rho}\|)\bar{\boldsymbol{z}}_2\right\} + \bar{\boldsymbol{z}}_2^{\mathrm{T}}\boldsymbol{M}^{-1}\hat{\boldsymbol{M}}\bar{\boldsymbol{\tau}} + \frac{1}{\gamma_\chi}[N_2(\chi_2)\Lambda_2 - 1]\dot{\chi}_2.
\end{aligned} \tag{38}$$

According to $\boldsymbol{Y}_2 = \boldsymbol{X}_d - \boldsymbol{\alpha}$, (17) and (18), the time derivative of $\boldsymbol{Y}_2$ is

$$\begin{aligned}
\dot{\boldsymbol{Y}}_2 &= \dot{\boldsymbol{X}}_d - \dot{\boldsymbol{\alpha}} \\
&= -\frac{\boldsymbol{Y}_2}{T_d} - \dot{\boldsymbol{\alpha}} \\
&= -\frac{\boldsymbol{Y}_2}{T_d} + \boldsymbol{B}\left(\boldsymbol{z}_1, \bar{\boldsymbol{z}}_2, \dot{\boldsymbol{\eta}}_\alpha, \ddot{\boldsymbol{\eta}}_\alpha, \boldsymbol{P}, \dot{\boldsymbol{P}}, \boldsymbol{Q}, \dot{\boldsymbol{Q}}\right),
\end{aligned} \tag{39}$$

where $\boldsymbol{B}(\boldsymbol{z}_1, \bar{\boldsymbol{z}}_2, \dot{\boldsymbol{\eta}}_\alpha, \ddot{\boldsymbol{\eta}}_\alpha, \boldsymbol{P}, \dot{\boldsymbol{P}}, \boldsymbol{Q}, \dot{\boldsymbol{Q}})$ is a continuous function vector.

According to (39) and Young's inequality, we have

$$\begin{aligned}
\boldsymbol{Y}_2^{\mathrm{T}}\dot{\boldsymbol{Y}}_2 &\le -\frac{\boldsymbol{Y}_2^{\mathrm{T}}\boldsymbol{Y}_2}{T_d} + \|\boldsymbol{Y}_2\|\left\|\boldsymbol{B}\left(\boldsymbol{z}_1, \bar{\boldsymbol{z}}_2, \dot{\boldsymbol{\eta}}_\alpha, \ddot{\boldsymbol{\eta}}_\alpha, \boldsymbol{P}, \dot{\boldsymbol{P}}, \boldsymbol{Q}, \dot{\boldsymbol{Q}}\right)\right\| \\
&\le -\frac{\boldsymbol{Y}_2^{\mathrm{T}}\boldsymbol{Y}_2}{T_d} + \frac{1}{2}\|\boldsymbol{Y}_2\|^2\left\|\boldsymbol{B}\left(\boldsymbol{z}_1, \bar{\boldsymbol{z}}_2, \dot{\boldsymbol{\eta}}_\alpha, \ddot{\boldsymbol{\eta}}_\alpha, \boldsymbol{P}, \dot{\boldsymbol{P}}, \boldsymbol{Q}, \dot{\boldsymbol{Q}}\right)\right\|^2 + \frac{1}{2}.
\end{aligned} \tag{40}$$

In the light of (33), we obtain

$$\begin{aligned}
\sum_{j=1}^{3} m_{j,j}^{-1}H_j^{-1}\tilde{m}_{j,j}\dot{\hat{m}}_{j,j} &= -\sum_{j=1}^{3} m_{j,j}^{-1}\tilde{m}_{j,j}\bar{\tau}_j z_{2,j} - \sum_{j=1}^{3}\frac{1}{2}m_{j,j}^{-1}\Omega_j\tilde{m}_{j,j}\hat{m}_{j,j} \\
&\le -\sum_{j=1}^{3} m_{j,j}^{-1}\tilde{m}_{j,j}\bar{\tau}_j z_{2,j} - \sum_{j=1}^{3}\frac{1}{2}m_{j,j}^{-1}\Omega_j\left(\tilde{m}_{j,j}^2 + \hat{m}_{j,j}^2 - m_{j,j}^2\right) \\
&\le -\sum_{j=1}^{3} m_{j,j}^{-1}\tilde{m}_{j,j}\bar{\tau}_j z_{2,j} - \sum_{j=1}^{3}\frac{1}{2}m_{j,j}^{-1}\Omega_j\tilde{m}_{j,j}^2 + \sum_{j=1}^{3}\frac{1}{2}m_{j,j}^{-1}\Omega_j m_{j,j}^2.
\end{aligned} \tag{41}$$

According to (34), we have

$$\begin{aligned}
\tilde{\Theta}\Gamma^{-1}\dot{\tilde{\Theta}} &= \tilde{\Theta}\phi^2(\|\boldsymbol{\rho}\|)\left\|\bar{\boldsymbol{z}}_2\right\|^2 - \frac{\sigma}{2}\tilde{\Theta}\hat{\Theta} \\
&= \tilde{\Theta}\phi^2(\|\boldsymbol{\rho}\|)\left\|\bar{\boldsymbol{z}}_2\right\|^2 - \frac{\sigma}{2}\left(\tilde{\Theta}^2 + \hat{\Theta}^2 - \Theta^{*2}\right) \\
&\le \tilde{\Theta}\phi^2(\|\boldsymbol{\rho}\|)\left\|\bar{\boldsymbol{z}}_2\right\|^2 - \frac{\sigma}{2}\tilde{\Theta}^2 + \frac{\sigma}{2}\Theta^{*2}.
\end{aligned} \tag{42}$$

Substituting (37)-(42) in (36) and rearranging, we have

$$\begin{aligned}\dot{V} \leq & -\boldsymbol{z}_1^{\mathrm{T}}\boldsymbol{K}_1\boldsymbol{z}_1 - \bar{\boldsymbol{z}}_2^{\mathrm{T}}\boldsymbol{I}\boldsymbol{K}_3\bar{\boldsymbol{z}}_2 + \frac{1}{2}\|\boldsymbol{Y}_2\|^2 + \frac{1}{2}K_2^2 + \frac{\Theta^*}{4} - \frac{\boldsymbol{Y}_2^T\boldsymbol{Y}_2}{T_d} \\ & + \frac{1}{2}\|\boldsymbol{Y}_2\|^2\left\|\boldsymbol{B}\left(\boldsymbol{z}_1, \bar{\boldsymbol{z}}_2, \dot{\boldsymbol{\eta}}_\alpha, \ddot{\boldsymbol{\eta}}_\alpha, \boldsymbol{P}, \dot{\boldsymbol{P}}, \boldsymbol{Q}, \dot{\boldsymbol{Q}}\right)\right\| + \frac{1}{2} - \sum_{j=1}^{3}\frac{1}{2}m_{j,j}^{-1}\Omega_j\tilde{m}_{j,j}^2 + \sum_{j=1}^{3}\frac{1}{2}m_{j,j}\Omega_j \\ & - \frac{\sigma}{2}\tilde{\Theta}^2 + \frac{\sigma}{2}\Theta^{*2} + \frac{1}{\gamma_\chi}\left[N_2(\chi_2)\Lambda_2 - 1\right]\dot{\chi}_2. \end{aligned} \tag{43}$$

Consider the sets $\boldsymbol{\Pi}_1 = \{\|\boldsymbol{\eta}_d\|^2 + \|\dot{\boldsymbol{\eta}}_d\|^2 + \|\ddot{\boldsymbol{\eta}}_d\|^2 + \|\bar{\boldsymbol{e}}\|^2 + \|\dot{\bar{\boldsymbol{e}}}\|^2 + \|\ddot{\bar{\boldsymbol{e}}}\|^2 + \|\underline{\boldsymbol{e}}\|^2 + \|\dot{\underline{\boldsymbol{e}}}\|^2 + \|\ddot{\underline{\boldsymbol{e}}}\|^2 \leq A_0, \forall A_0 > 0\}$ and $\boldsymbol{\Pi}_2 = \{(\boldsymbol{z}_1, \bar{\boldsymbol{z}}_2, \boldsymbol{Y}_2, \tilde{\boldsymbol{M}}, \tilde{\Theta}) : V \leq B_0, \forall B_0 > 0\}$. Then, the two-norm $\|\boldsymbol{B}(\cdot)\|$ of the continue function vector $\boldsymbol{B}(\cdot)$ in (39) has the maximum B_M on $\boldsymbol{\Pi}_1 \times \boldsymbol{\Pi}_2$. Choosing $\frac{1}{T_d} = \frac{1}{2} + \frac{B_M^2}{2} + \mu^*$ with μ^* being a positive constant, we have

$$\begin{aligned}\dot{V} \leq & -\boldsymbol{z}_1^T\boldsymbol{K}_1\boldsymbol{z}_1 - \bar{\boldsymbol{z}}_2^T\boldsymbol{I}\boldsymbol{K}_3\bar{\boldsymbol{z}}_2 - \mu^*\|\boldsymbol{Y}_2\|^2 - \sum_{j=1}^{3}\frac{1}{2}m_{j,j}^{-1}\Omega_j\tilde{m}_{j,j}^2 - \frac{\sigma}{2}\tilde{\Theta}^2 + \frac{1}{2}K_2^2 + \frac{1}{2} + \frac{\Theta^*}{4} + \frac{\sigma}{2}\Theta^{*2} \\ & + \sum_{j=1}^{3}\frac{1}{2}m_{j,j}\Omega_j - \left(1 - \frac{\|\boldsymbol{B}(\cdot)\|^2}{B_M^2}\right)\frac{B_M^2\|\boldsymbol{Y}_2\|^2}{2} + \frac{1}{\gamma_\chi}\left[N_2(\chi_2)\Lambda_2 - 1\right]\dot{\chi}_2 \\ \leq & -\lambda_{\min}(\boldsymbol{K}_1)\boldsymbol{z}_1^{\mathrm{T}}\boldsymbol{z}_1 - \lambda_{\min}(\boldsymbol{I}\boldsymbol{K}_3)\bar{\boldsymbol{z}}_2^{\mathrm{T}}\bar{\boldsymbol{z}}_2 - \sum_{j=1}^{3}\frac{1}{2}m_{j,j}^{-1}\Omega_j\tilde{m}_{j,j}^2 - \frac{\sigma}{2}\tilde{\Theta}^2 + \frac{1}{2}K_2^2 + \frac{1}{2} + \frac{\Theta^*}{4} + \frac{\sigma}{2}\Theta^{*2} \\ & + \sum_{j=1}^{3}\frac{1}{2}m_{j,j}\Omega_j - \left(1 - \frac{\|\boldsymbol{B}(\cdot)\|^2}{B_M^2}\right)\frac{B_M^2\|\boldsymbol{Y}_2\|^2}{2} + \frac{1}{\gamma_\chi}\left[N_2(\chi_2)\Lambda_2 - 1\right]\dot{\chi}_2 \\ \leq & -2\mu V + C - \left(1 - \frac{\|\boldsymbol{B}(\cdot)\|^2}{B_M^2}\right)\frac{B_M^2\|\boldsymbol{Y}_2\|^2}{2} + \frac{1}{\gamma_\chi}\left[N_2(\chi_2)\Lambda_2 - 1\right]\dot{\chi}_2 \\ \leq & -2\mu V + C + \frac{1}{\gamma_\chi}\left[N_2(\chi_2)\Lambda_2 - 1\right]\dot{\chi}_2, \end{aligned} \tag{44}$$

where μ and C are

$$\mu = \min\left\{\lambda_{\min}(\boldsymbol{K}_1), \lambda_{\min}(\boldsymbol{I}\boldsymbol{K}_3), \min\left(\Omega_j H_j\right), \frac{\sigma}{2}\Gamma\right\}, C = \frac{1}{2}K_2^2 + \sum_{j=1}^{3}\frac{1}{2}m_j\Omega_j + \frac{1}{2} + \frac{\Theta^*}{4} + \frac{\sigma}{2}\Theta^*. \tag{45}$$

The aforementioned main results are summarized in the following theorem.

Theorem 1. *Considering the closed-loop system consisting of the AUV (1)-(2) under Assumption 1, the tracking control law (32) with the adaptive laws (33) and (34), the virtual control (17), and the additional control in (25) with the auxiliary dynamic system (26). Under the condition $-\underline{e}_j(0) < e_j(0) < \bar{e}_j(0)$, the actual trajectory $\boldsymbol{\eta}$ of the AUV tracks the desired trajectory $\boldsymbol{\eta}_d$ with the prescribed control performance (6) by artfully adjusting the design parameters $\boldsymbol{K}_1$, K_2, $\boldsymbol{K}_3$, γ, γ_χ, H, Ω, Γ, σ, and the tracking error satisfies the prescribed performance (5). All signals of the AUV trajectory tracking closed-loop control system are guaranteed to be uniformly ultimately bounded.*

Proof. Solving (45), we have

$$0 \leq V(t) \leq \frac{C}{2\mu} + \left[V(0) - \frac{C}{2\mu}\right]\exp^{-2\mu t} + \frac{\exp^{-2\mu t}}{\gamma_\chi}\int_0^t (N_2(\chi_2)\Lambda_2 - 1)\dot{\chi}_2\exp^{2\mu s}ds. \tag{46}$$

From (46) and Lemma 1, it is obviously seen that $V(t)$ and χ_2 are uniformly ultimately bounded for all $V(0) \leq B_0$. Therefore, we know from (35) that $\|\boldsymbol{z}_1\|$, $\|\bar{\boldsymbol{z}}_2\|$, $\tilde{m}_{j,j}$, and $\tilde{\Theta}$ are bounded for all $V(0) \leq B_0$. Furthermore, we can know from (4), (17), $\boldsymbol{Y}_2 = \boldsymbol{X}_d - \boldsymbol{\alpha}$, (25) and the boundness of $\tanh(\lambda_2)$, $m_{j,j}$, and Θ that $\boldsymbol{\eta}$, $\boldsymbol{\alpha}$, $\boldsymbol{X}_d$, $\boldsymbol{v}$, $\hat{m}_{j,j}$, and $\hat{\Theta}$ are uniformly

ultimately bounded for all $V(0) \leq B_0$. From the property of the error mapping function (14), the tracking error satisfies the prescribed performance (6). Hence, the position of the AUV $\boldsymbol{\eta}$ tracks the desired trajectory $\boldsymbol{\eta}_d$ with arbitrarily small error by appropriately adjusting the design parameters. Furthermore, according to (27), (38), and (47) (see the work of Wen et al,[37]

$$|\Lambda_2 \lambda_2| = \left| \frac{4\lambda_2}{(e^{\lambda_2} + e^{-\lambda_2})^2} \right| \leq \frac{1}{2}. \tag{47}$$

$\|\bar{\boldsymbol{\xi}}\|$ is bounded. This implies that $\|\boldsymbol{\xi}\|$ in (27) is bounded due to the boundedness of χ_2, then $\|\boldsymbol{\lambda}\|$ are bounded from (26). Thus, all signals in the closed-loop control system are uniformly ultimately bounded. Theorem 1 is proved. □

4 | SIMULATIONS

In this section, in order to demonstrate the effectiveness of the proposed robust adaptive trajectory tracking control scheme, we carry out the simulations on an AUV from the work of Cui et al in two cases and compare our proposed control law with the law without the prescribed performance. The dynamic parameters of the AUV are given by $m_{1,1} = 200$ kg, $m_{2,2} = 250$ kg, $m_{3,3} = 80$ kg, $d_{1,1} = (70 + 100|u|)$ kg $\cdot$ s^{-1}, $d_{2,2} = (100 + 200|v|)$ kg $\cdot$ s^{-1}, and $d_{3,3} = (50 + 100|r|)$ kg $\cdot$ s^{-1}.

4.1 | Performance of proposed trajectory tracking control law

In this section, to verify the adaptability and the robustness of the developed control scheme, we do simulations in the following two cases.

Case 1. The desired trajectory $\eta_d = [x_d, y_d, \psi_d]^{\mathrm{T}}$ is given by

$$x_d = 0.5t, y_d = 10\sin(0.004\pi t), \psi_d = \operatorname{atan}(y_d/x_d). \tag{48}$$

The disturbance vector[4] in the body frame is given by

$$\boldsymbol{d}(t) = \boldsymbol{J}^{\mathrm{T}}(\psi) \begin{bmatrix} 10 + 1.8\sin(0.7t) + 1.2\sin(0.05t) + 1.2\sin(0.9t) \\ 5 + 0.4\sin(0.1t) + 0.2\cos(0.6t) \\ 0 \end{bmatrix}. \tag{49}$$

The following initial conditions and control law design parameters are adopted in the simulation $\boldsymbol{\eta}_d(0) = [0, 0, \pi/4]^{\mathrm{T}}$, $\boldsymbol{\upsilon}_d(0) = [0, 0, 0]^{\mathrm{T}}$; $\boldsymbol{\eta}(0) = [-2, 2, 0]^{\mathrm{T}}$, $\boldsymbol{\upsilon}(0) = [0, 0, 0]^{\mathrm{T}}$; $\hat{\Theta}(0) = 0$, $\hat{\boldsymbol{M}}(0) = \operatorname{diag}(200, 50, 20)$, $\boldsymbol{K}_1 = \operatorname{diag}(0.01, 0.01, 4)$, $K_2 = 50$, $\boldsymbol{K}_3 = \begin{bmatrix} 50 & 40 & 0 \\ -40 & 50 & -40 \\ 0 & 40 & 30 \end{bmatrix}$, $\Gamma = 200, \sigma = 0.001, \gamma = 50, \gamma_\chi = 0.1, H_1 = H_2 = H_3 = 200$, $\Omega_1 = \Omega_2 = \Omega_3 = 0.01$. The prescribed boundaries of the tracking errors are $\bar{e}_1(t) = 0.9\exp(-0.1t) + 0.1$, $\underline{e}_1(t) = 2.9\exp(-0.1t) + 0.1$, $\bar{e}_2(t) = 2.9\exp(-0.1t) + 0.1$, $\underline{e}_2(t) = 0.9\exp(-0.1t) + 0.1$, $\bar{e}_3(t) = 0.96\exp(-0.1t) + 0.04$, and $\underline{e}_3(t) = 0.46\exp(-0.1t) + 0.04$, receptively.

The simulation results are plotted using the solid lines in Figures 2A to 2I. The quantitative performance indices are summarized in Table 1, where the settling times of the tracking errors e_x, e_y, and e_ψ are taken as the times at which the tracking errors arrive at and stay within the allowed tolerance 0.1 m, 0.1 m, and 0.04 rad, respectively. It can be obviously seen from Figures 2A and 2B and Table 1 that the AUV can track the desired trajectory (48) with the prescribed tracking performance. Figure 2C shows that the control inputs τ_u and τ_r are reasonable. Figures 2F to 2I show that the estimation $\hat{\Theta}$ of Θ, the estimations $\hat{m}_{1,1}$ and $\hat{m}_{3,3}$ of $m_{1,1}$ and $m_{3,3}$, and Nussbaum gain $N(\chi_2)$ and its parameter χ_2 are all bounded. The aforementioned simulation results are as the Theorem 1 proved.

Case 2. Consider the masses of the AUV are perturbed by 10% around the nominal values. The desired trajectory and the design parameters are the same as those in Case 1, and a more general and bigger external disturbance vector is chosen in this case

$$\boldsymbol{d}(t) = \boldsymbol{J}^{\mathrm{T}}(\psi) \begin{bmatrix} 14 + \sin(0.8t + \pi/8) - 0.5\sin(0.5\pi t) \\ 8 + 1.2\sin(0.8t + \pi/8) + 0.6\sin(0.6\pi t) \\ 3 + \sin(0.8t + \pi/6) - 0.5\sin(0.3\pi t) \end{bmatrix}. \tag{50}$$

The simulation results are presented in Figures 3A to 3G. It can be seen that the developed robust adaptive tracking control law exhibits similar control performance to that in Case 1, which shows that the developed prescribed

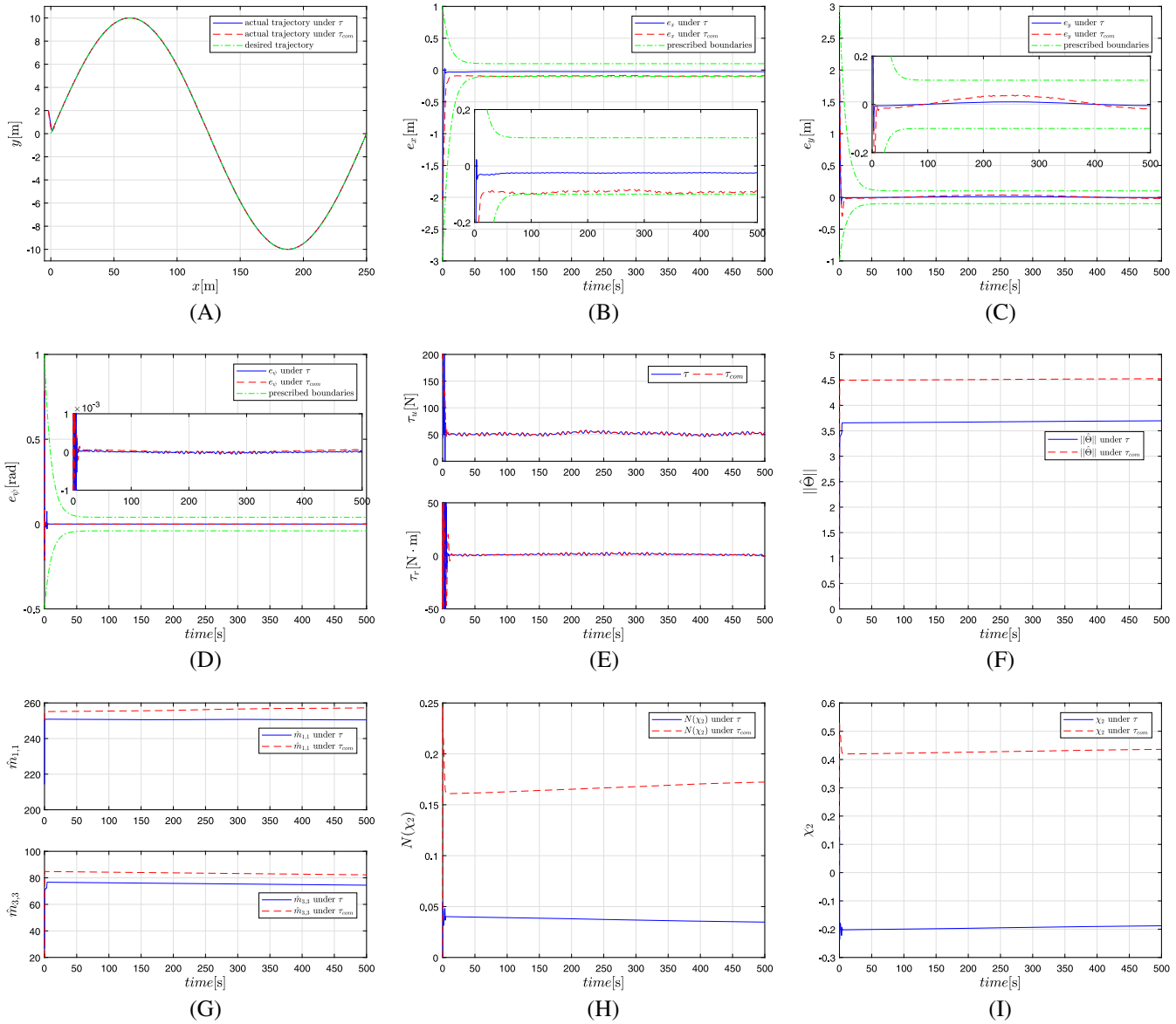

FIGURE 2 A, Actual and desired trajectories of the AUV; B, Tracking error e_x; C, Tracking error e_y; D, Tracking error e_ψ; E, Control inputs; F, Estimation $\hat{\Theta}$ of Θ; G Estimations $\hat{m}_{1,1}$ and $\hat{m}_{3,3}$ of $m_{1,1}$ and $m_{3,3}$; H, Nussbaum function $N(\chi_2)$; I, Adapting parameter χ_2. AUV, autonomous underwater vehicle [Colour figure can be viewed at wileyonlinelibrary.com]

performance tracking control law for the AUV has the adaptability and the robustness in the presence of unknown dynamic parameters and time-varying disturbances.

Remark 7. In the simulations, through trial and error, we firstly choose design parameters $\boldsymbol{K}_1$, satisfying $\lambda_{\min}(\boldsymbol{K}_1) > 0$ and $\boldsymbol{K}_3$, whose each element should be positive to ensure that the system is stable. Furthermore, we properly regulate the other design parameters K_2, γ, γ_χ, H_j, Ω_j, Γ, and σ to get the satisfactory control performance. Parameters $\bar{e}_{j,0}$ and $\underline{e}_{j,0}$ of the prescribed boundaries are chosen large enough to ensure $-\underline{e}_j(0) < e_j(0) < \bar{e}_j(0)$. μ_j prescribes the convergence speed of the tracking errors. The larger μ_j is, the faster the tracking errors converge. The parameters $\bar{e}_{j,\infty}$ prescribe the steady-state performance of the tracking errors and are usually chosen as $0.05e_j(0)$.

We have done an amount of simulations in many scenarios, which shows that the larger parameters $\boldsymbol{K}_1$, $\boldsymbol{K}_3$, H_j, and σ are, the higher the control accuracy is and the larger the control signal is. In fact, the resulting tracking performance is related to all the parameters, therefore it is needed to comprehensively tune all the parameters together, instead of separately tuning individual parameters.

TABLE 1 Performance indices in two cases

	Case 1		Case 2	
Performance indices	τ	τ_{com}	τ	τ_{com}
Settling time of e_x	2.63 s	11.56 s	2.66 s	12.79 s
Settling time of e_y	2.92 s	6.45 s	2.08 s	6.51 s
Settling time of e_ψ	3.84 s	0.40 s	3.91 s	1.97 s
$\int_0^{500} \|\|e\|\| dt$	15.2	50.40	15.77	54.03

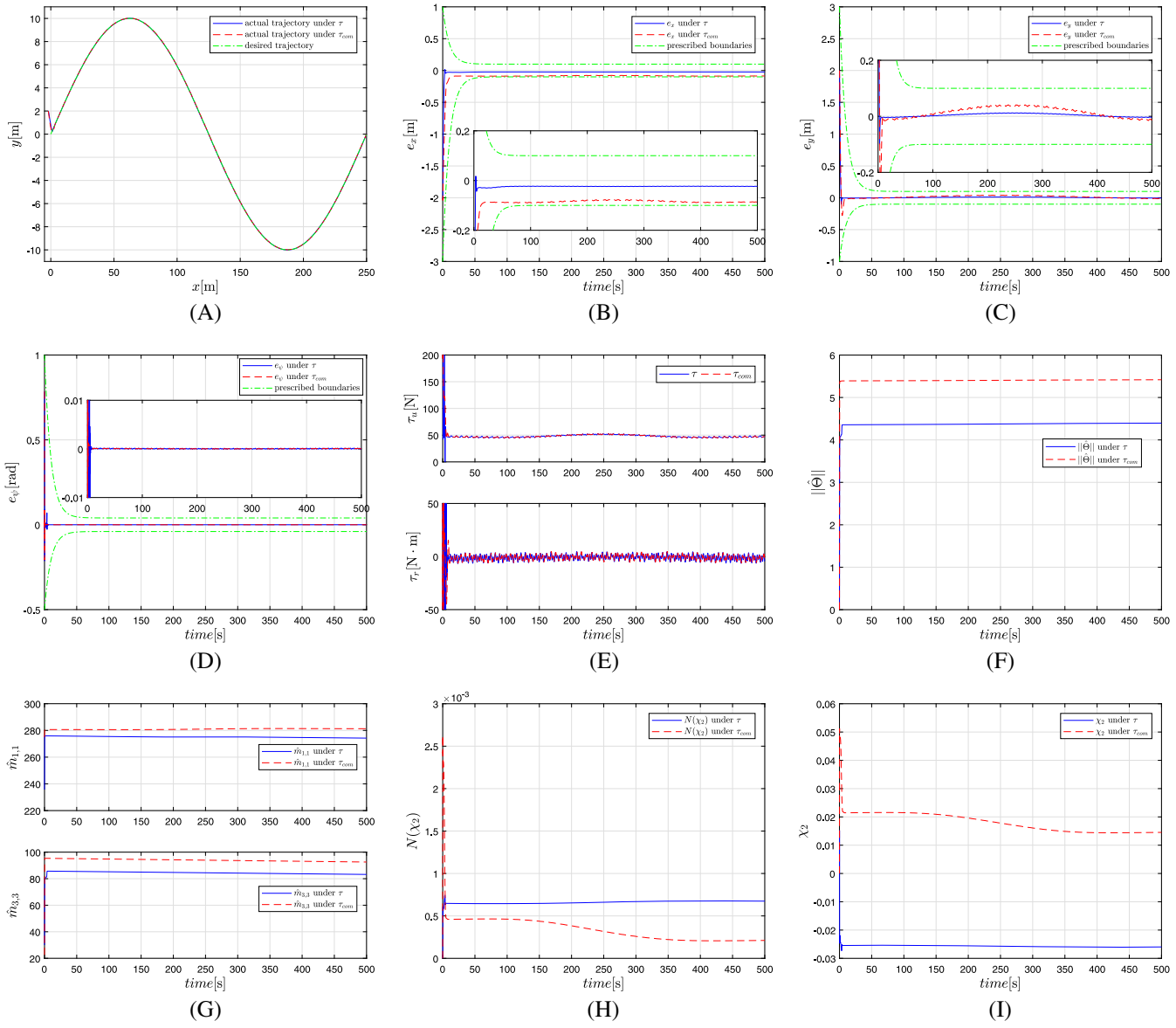

FIGURE 3 A, Actual and desired trajectories of the AUV; B, Tracking error e_x; C, Tracking error e_y; D, Tracking error e_ψ; E, Control inputs; F, Estimation $\hat{\Theta}$ of Θ; G, Estimations $\hat{m}_{1,1}$ and $\hat{m}_{3,3}$ of $m_{1,1}$ and $m_{3,3}$; H, Nussbaum function $N(\chi_2)$; I, Adapting parameter χ_2. AUV, autonomous underwater vehicle [Colour figure can be viewed at wileyonlinelibrary.com]

4.2 | Simulation comparison

In this section, we compare our proposed control law with the following control law without the prescribed performance in Case 1 and Case 2, ie,

$$\boldsymbol{\tau}_{\text{com}} = \hat{\boldsymbol{M}}_{\text{com}} \boldsymbol{L}_2 \left[-\boldsymbol{J}^{\text{T}}(\psi)\boldsymbol{e} - \boldsymbol{K}_3 \bar{\boldsymbol{z}}_{2,\text{com}} - \hat{\Theta}_{\text{com}} \phi^2(\boldsymbol{\rho}) \bar{\boldsymbol{z}}_{2,\text{com}} \right], \tag{51}$$

with the intermediate control vector $\boldsymbol{\alpha}_{\text{com}}$

$$\boldsymbol{\alpha}_{\text{com}} = \boldsymbol{J}^{\text{T}}(\psi)\left(-\boldsymbol{K}_1\boldsymbol{e}_1 + \dot{\boldsymbol{\eta}}_{\alpha}\right) \tag{52}$$

and the adaptive laws

$$\dot{\hat{m}}_{\text{com},j,j} = -H_j\left(\overline{\tau}_{\text{com},j}\overline{z}_{2,\text{com},j} + \Omega_j\hat{m}_{\text{com},j,j}\right), j = 1,2,3 \tag{53}$$

$$\dot{\hat{\Theta}}_{\text{com}} = \Gamma\left[\phi^2(\|\boldsymbol{\rho}\|)\left\|\overline{\boldsymbol{z}}_{2,\text{com}}\right\|^2 - \sigma\hat{\Theta}_{\text{com}}\right], \tag{54}$$

where $\overline{\boldsymbol{\tau}}_{\text{com}} = \left[\overline{\tau}_{\text{com},1}, \overline{\tau}_{\text{com},2}, \overline{\tau}_{\text{com},3}\right]^{\text{T}} = \boldsymbol{L}_2\left[-\boldsymbol{J}^{\text{T}}(\psi)\boldsymbol{e} - \boldsymbol{K}_3\overline{\boldsymbol{z}}_{2,\text{com}} - \hat{\Theta}_{\text{com}}\phi^2(\boldsymbol{\rho})\overline{\boldsymbol{z}}_{2,\text{com}}\right]$.

The desired trajectories, disturbance vectors, initial conditions, and related control law design parameters are taken the same as those in two cases in Section 4.1. The simulation results under $\boldsymbol{\tau}_{\text{com}}$ are depicted using the dashed lines in Figures 2A to 2I and Figures 3A to 3I, respectively. Furthermore, the performance indices are also summarized in Table 1. It is obviously seen from Figures 2A and 2B, Figures 3A and 3B, and Table 1 that our proposed robust trajectory tracking control law $\boldsymbol{\tau}$ exhibits better control performances than the control law $\boldsymbol{\tau}_{\text{com}}$ in both Case 1 and Case 2.

5 | CONCLUSIONS

In the simultaneous presence of unknown dynamic parameters and disturbances, the problem of trajectory tracking control for underactuated AUV with prescribed performance has been solved in this paper. A novel additional control is proposed to deal with the underactuation of the AUV. Based on a simple error mapping function, a robust adaptive prescribed performance trajectory tracking control law was designed using the DSC technique. Stability analysis and simulation results have demonstrated the effectiveness of the developed trajectory tracking control scheme. Furthermore, the developed control scheme can be applied to the prescribed performance tracking control of a wide range of nonholonomic MIMO systems with unknown dynamic parameters and disturbances.

ORCID

Jian Li https://orcid.org/0000-0003-3738-2551
Jialu Du https://orcid.org/0000-0002-9809-0862

REFERENCES

1. Wynn RB, Huvenne VAI, Le Bas TPL, et al. Autonomous underwater vehicles (AUVs): their past, present and future contributions to the advancement of marine geoscience. *Marine Geology*. 2014;352:451-468.
2. Batista P, Silvestre C, Oliveira P. A two-step control approach for docking of autonomous underwater vehicles. *Int J Robust Nonlinear Control*. 2014;25(10):1528-1547.
3. dos Santos CHF, Cildoz MU, Vieira RP, Reginatto R, Pinheiro BC. Nonlinear mapping for performance improvement and energy saving of underwater vehicles. *Int J Robust Nonlinear Control*. 2018;28(18):5811-5840.
4. Cui RX, Ge SS, How BVE, Choo YS. Leader-follower formation control of underactuated autonomous underwater vehicles. *Ocean Engineering*. 2010;37:1491-1502.
5. Alonge F, D'Ippolito F, Raimondi FM. Trajectory tracking of underactuated underwater vehicles. In: Proceedings of the 40th IEEE Conference on Decision and Control; 2001; Orlando, FL.
6. Antonelli G, Chiaverini S, Sarkar N, West M. Adaptive control of an autonomous underwater vehicle: experimental results on ODIN. *IEEE Trans Control Syst Technol*. 2001;9(5):756-765.
7. Bartolini G, Pisano A. Black-box position and attitude tracking for underwater vehicles by second-order sliding-mode technique. *Int J Robust Nonlinear Control*. 2018;20(14):1594-1609.
8. Shen C, Shi Y, Buckham B. Integrated path planning and tracking control of an AUV: a unified receding horizon optimization approach. *IEEE/ASME Trans Mechatron*. 2017;22(3):1163-1173.
9. Antonelli G, Caccavale F, Chiaverini S, Fusco G. A novel adaptive control law for underwater vehicles. *IEEE Trans Control Syst Technol*. 2003;11(2):221-232.

10. Zhang MJ, Liu X, Yin BJ, Liu WX. Adaptive terminal sliding mode based thruster fault tolerant control for underwater vehicle in time-varying ocean currents. *J Franklin Inst*. 2015;352(11):4935-4961.
11. Qiao L, Zhang WD. Adaptive non-singular integral terminal sliding mode tracking control for autonomous underwater vehicles. *IET Control Theory Appl*. 2017;11(8):1293-1306.
12. Miao BB, Li TS, Luo WL. A DSC and MLP based robust adaptive NN tracking control for underwater vehicle. *Neurocomputing*. 2013;111(6):184-189.
13. Wang YJ, Zhang MJ, Wilson PA, Liu X. Adaptive neural network-based backstepping fault tolerant control for underwater vehicles with thruster fault. *Ocean Engineering*. 2015;110:15-24.
14. Fischer N, Hughes D, Walters P, Schwartz EM, Dixon WE. Nonlinear RISE-based control of an autonomous underwater vehicle. *IEEE Trans Robotics*. 2014;30(4):845-852.
15. Liu SY, Liu YJ, Wang N. Nonlinear disturbance observer-based backstepping finite-time sliding mode tracking control of underwater vehicles with system uncertainties and external disturbances. *Nonlinear Dynamics*. 2017;88(1):465-476.
16. Li SH, Wang XY, Zhang LJ. Finite-time output feedback tracking control for autonomous underwater vehicles. *IEEE J Ocean Eng*. 2015;40(3):727-751.
17. Park BS. Neural network-based tracking control of underactuated autonomous underwater vehicles with model uncertainties. *J Dyn Syst Meas Control*. 2015;137:1-7.
18. Elmokadem T, Zribi M, Youcef-Toumi K. Terminal sliding mode control for the trajectory tracking of underactuated autonomous underwater vehicles. *Ocean Engineering*. 2016;129:613-625.
19. Yu CY, Xiang XB, Zhang Q, Xu GH. Adaptive fuzzy trajectory tracking control of an under-actuated autonomous underwater vehicle subject to actuator saturation. *Int J Fuzzy Syst*. 2017;20(1):269-279.
20. Shojaei K, Arefi MM. On the neuro-adaptive feedback linearising control of underactuated autonomous underwater vehicles in three-dimensional space. *IET Control Theory Appl*. 2015;9(8):1264-1273.
21. Shojaei K, Dolatshahi M. Line-of-sight target tracking control of underactuated autonomous underwater vehicles. *Ocean Engineering*. 2017;133:244-252.
22. Do KD, Pan J, Jiang ZP. Robust and adaptive path following for underactuated autonomous underwater vehicles. *Ocean Engineering*. 2004;31(16):1967-1997.
23. Xiang XB, Yu CY, Zhang Q. Robust fuzzy 3D path following for autonomous underwater vehicle subject to uncertainties. *Comput Oper Res*. 2016;84:165-177.
24. Caharija W, Pettersen KY, Bibuli M, et al. Integral line-of-sight guidance and control of underactuated marine vehicles: theory, simulations, and experiments. *IEEE Trans Control Syst Technol*. 2016;24(5):1623-1642.
25. Bechlioulis CP, Rovithakis GA. Robust adaptive control of feedback linearizable MIMO nonlinear systems with prescribed performance. *IEEE Trans Autom Control*. 2008;53(9):2090-2099.
26. Wang XJ, Yin XH, Shen F. Disturbance observer based adaptive neural prescribed performance control for a class of uncertain nonlinear systems with unknown backlash-like hysteresis. *Neurocomputing*. 2018;299:10-19.
27. Li YM, Tong SC. Adaptive fuzzy control with prescribed performance for block-triangular-structured nonlinear systems. *IEEE Trans Fuzzy Syst*. 2018;26(3):1153-1163.
28. Wang W, Wang D, Peng ZH, Li TS. Prescribed performance consensus of uncertain nonlinear strict-feedback systems with unknown control directions. *IEEE Trans Syst Man Cybern Syst*. 2016;46(9):1279-1286.
29. Bechlioulis CP, Kyriakopoulos KJ. Robust prescribed performance tracking control for unknown underactuated torpedo-like AUVs. Paper presented at: 2013 European Control Conference (ECC); 2013; Zurich, Switzerland.
30. Bechlioulis CP, Karras GC, Heshmati-Alamdari S, Kyriakopoulos KJ. Trajectory tracking with prescribed performance for underactuated underwater vehicles under model uncertainties and external disturbances. *IEEE Trans Control Syst Technol*. 2017;25(2):429-440.
31. Elhaki O, Shojaei K. Neural network-based target tracking control of underactuated autonomous underwater vehicles with a prescribed performance. *Ocean Engineering*. 2018;167:239-256.
32. Park BS, Yoo SJ. Robust fault-tolerant tracking with predefined performance for underactuated surface vessels. *Ocean Engineering*. 2016;115:159-167.
33. He SD, Wang M, Dai SL, Luo F. Leader-follower formation control of USVs with prescribed performance and collision avoidance. *IEEE Trans Ind Inform*. 2019;15(1):572-581.
34. Han SI, Lee JM. Recurrent fuzzy neural network backstepping control for the prescribed output tracking performance of nonlinear dynamic systems. *ISA Transactions*. 2014;53(1):33-43.
35. Wang CC, Yang GH. Observer-based adaptive prescribed performance tracking control for nonlinear systems with unknown control direction and input saturation. *Neurocomputing*. 2018;284:17-26.
36. Nussbaum RD. Some remarks on a conjecture in parameter adaptive control. *Syst Control Lett*. 1983;3(5):243-246.
37. Wen CY, Zhou J, Liu ZT, Su HY. Robust adaptive control of uncertain nonlinear systems in the presence of input saturation and external disturbance. *IEEE Trans Autom Control*. 2011;56(7):1672-1678.
38. Ryan EP. A universal adaptive stabilizer for a class of nonlinear systems. *Syst Control Lett*. 1991;16(3):209-218.
39. Swaroop D, Hedrick JK, Yip PP, Gerdes JC. Dynamic surface control for a class of nonlinear systems. *IEEE Trans Autom Control*. 2000;45(10):1893-1899.
40. Zhu GB, Du JL. Global robust adaptive trajectory tracking control for surface ships under input saturation. *J Ocean Eng*. 2018. Early access. https://doi.org/10.1109/JOE.2018.2877895

41. Wang QL, Psillakis HE, Sun CY. Cooperative control of multiple agents with unknown high-frequency gain signs under unbalanced and switching topologies. *IEEE Trans Autom Control*. 2019;64(6):2495-2501. https://doi.org/10.1109/TAC.2018.2867161
42. Wang QL, Sun CY. Adaptive consensus of multiagent systems with unknown high-frequency gain signs under directed graphs. *IEEE Trans Syst Man Cybern Syst*. 2018. Early access. https://doi.org/10.1109/TSMC.2018.2810089

How to cite this article: Li J, Du J, Sun Y, Lewis FL. Robust adaptive trajectory tracking control of underactuated autonomous underwater vehicles with prescribed performance. *Int J Robust Nonlinear Control*. 2019;1–15. https://doi.org/10.1002/rnc.4659